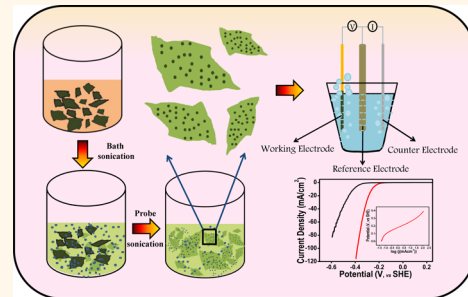


MoS₂ Quantum Dot-Interspersed Exfoliated MoS₂ Nanosheets

Deepesh Gopalakrishnan, Dijo Damien, and Manikoth M. Shaijumon*

Indian Institute of Science Education and Research Thiruvananthapuram, CET Campus, Sreekaryam, Thiruvananthapuram, Kerala, India, 695016

ABSTRACT We report the synthesis of heterodimensional nanostructures of MoS₂ quantum dots interspersed in few-layered sheets of MoS₂, using a liquid exfoliation technique in organic solvents. This unique hybrid morphology results from the optimized experimental conditions involving bath sonication followed by ultrasound probe sonication. We show that such heterodimensional hybrid materials could easily be extracted from the solvent as precipitates when post-treated with less polar volatile solvents such as chloroform. Such tailored MoS₂ nanostructures, when directly used as electrodes for hydrogen evolution reaction, showed excellent electrocatalytic activity with low overpotential. Hence, we believe this could lead to large-scale synthesis of liquid-exfoliated layered nanostructures for their potential applications.



KEYWORDS: MoS₂ · liquid exfoliation · quantum dots · nanosheets · hydrogen evolution reaction

Recent developments in two-dimensional layered inorganic materials such as monolayer and few-layer sheets of molybdenum disulfide (MoS₂), hexagonal boron nitride (hBN), and other dichalcogenides have shown great promise and are being investigated with great attention.^{1,2} Wide interest in such exfoliated materials including graphene, one of the intensely researched 2D crystals recently, results from their unique properties upon exfoliation.^{3–5} While graphene, with its zero band-gap energy, seems to be unsuitable for many electronics and optics applications, its recently explored inorganic analogues such as MoS₂, with its large intrinsic band gap and high carrier mobility, show great promise for such applications and have opened up new prospects for technological breakthroughs.⁶ Several recent studies have shown band-gap tuning of MoS₂ with layer thickness, from 1.2 eV indirect band gap for bulk material to a direct gap semiconductor with a 1.9 eV band gap for a single-layer MoS₂.⁷ The emerging strong photoluminescence in ultrathin MoS₂ layers while comparing with the absence of luminescence in the bulk is an indication of the transition from indirect band gap to direct band gap.⁸ This unique property results from the modified electronic properties,

and these materials have thus been explored for different applications in electronics, thermoelectrics, energy storage, gas sensing, catalysis, etc. Recently, several studies have sought to explore the high catalytic behavior of nanostructured MoS₂ for hydrogen evolution reaction (HER).^{9–16} However, the limited surface area, electrical conductivity, and, more importantly, the exposure of active edges of MoS₂ nanostructures still remain a challenge in using MoS₂-based catalysts for efficient evolution of hydrogen. Several approaches, for example, utilization of a graphene support¹³ and making porous MoS₂ thin films,¹¹ have been demonstrated to achieve enhanced HER kinetics for MoS₂-based catalysts.

Different methods to obtain few-layered MoS₂ have been reported, which include mechanical exfoliation,¹⁷ liquid exfoliation,^{1,18,19} chemical route,²⁰ and chemical vapor deposition (CVD).^{21,22} A liquid exfoliation technique reported by Coleman *et al.* through ultrasound sonication^{19,23} using organic solvents yielded few-layered sheets of MoS₂, while a bath sonication method has been shown to produce MoS₂ quantum dots from bulk MoS₂. A mixed solvent method has been demonstrated for the exfoliation of layered materials using volatile solvents. However, materials extraction from such

* Address correspondence to shaiju@iisertvm.ac.in.

Received for review March 16, 2014 and accepted April 28, 2014.

Published online April 28, 2014
10.1021/nn501479e

© 2014 American Chemical Society

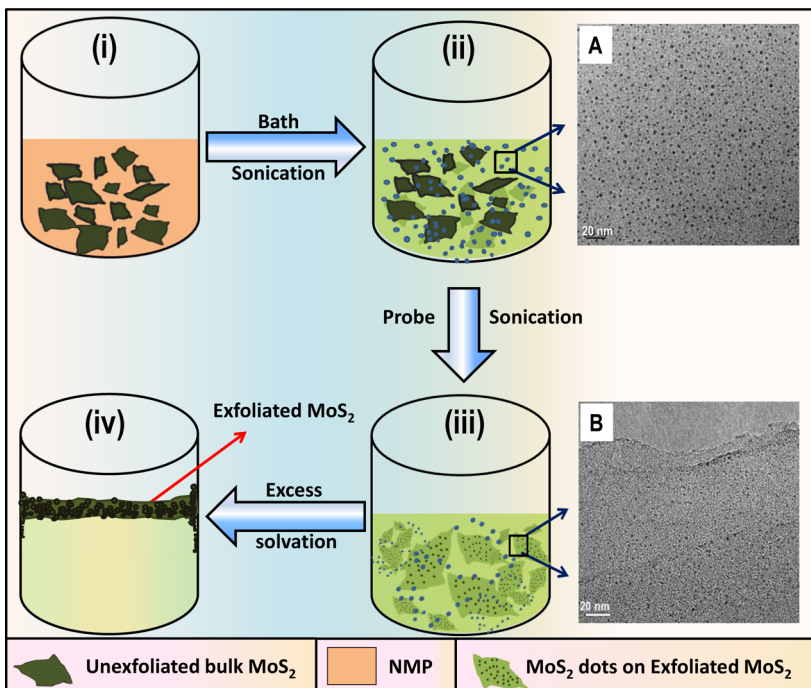


Figure 1. Schematic representation of the synthesis procedure to obtain MoS_2 quantum dots interspersed in MoS_2 nanosheets using a liquid exfoliation approach in 1-methyl-2-pyrrolidone solution. TEM images of (a) MoS_2 quantum dots of size ~ 2 nm formed through the bath sonication process and (b) MoS_2 quantum dots interspersed in the exfoliated MoS_2 nanosheets.

liquid dispersions without layer aggregation for further applications still remains a challenge. Hence it is important to modify the liquid exfoliation techniques to obtain a large concentration of few-layered MoS_2 nanosheets dispersed in appropriate solvents that allow easy extraction as precipitates. Here we report the synthesis of MoS_2 quantum dots interspersed within few-layered sheets of MoS_2 using a liquid exfoliation technique in organic solvents, through optimized experimental conditions involving bath sonication followed by ultrasound probe sonication. We show that such heterodimensional hybrid materials could easily be extracted from the solvent as precipitates when post-treated with less polar volatile solvents such as chloroform. We studied the HER performance of these hybrid nanostructures and found that they exhibit excellent electrocatalytic activity with low overpotential, mainly attributed to the large number of exposed active edges of MoS_2 .

RESULTS AND DISCUSSION

A highly dispersed suspension of MoS_2 quantum dots interspersed in few-layered MoS_2 nanosheets was prepared using a simple liquid exfoliation technique involving a combination of bath sonication followed by ultrasound probe sonication of MoS_2 flakes in 1-methyl-2-pyrrolidone (NMP), as schematically depicted in Figure 1. More details on the synthesis procedure is given in the Methods section. Bath sonication of MoS_2 flakes in NMP for 3.5 h results in the

formation of MoS_2 quantum dots (Figure 1A). The hydrodynamic forces resulting from the increased pressure and temperature during the bath sonication process lead to the breakdown of bulk MoS_2 into smaller particles in the solution. Formation of such nanoclusters is well understood.²⁴ Exfoliation of MoS_2 flakes into few-layered nanosheets using a probe sonication method has been reported by several research groups.¹⁹ Use of an ultrasonic horn results in the cleavage of bulk layers into ultrathin sheets (Figure S1, Supporting Information). Here, a combination of the two methods has been followed to obtain a disperse solution of heterodimensional nanostructures of MoS_2 quantum dots interspersed in few-layered MoS_2 nanosheets (Figure 1B). The high-resolution TEM (HRTEM) image clearly shows MoS_2 quantum dots of ~ 2 nm uniformly spread on the exfoliated sheets of MoS_2 (Figure 2A). The nanosheets are of larger lateral size ($1\ \mu\text{m}$). The particle size distribution given in Figure 2B shows that particles with varying size from ~ 0.5 to 4.5 nm with a maximum around 2.5 nm were obtained through this technique. It is also found that particles tend to slightly agglomerate with time; the size of particle reaches ~ 10 nm after 7 days, if the sample is kept undisturbed (Figure S2-A, Supporting Information). To further confirm the morphology and thickness of the as-formed MoS_2 quantum dots and the underlying nanosheets, atomic force microscopy (AFM) topography images of these nanostructures were analyzed (Figure 2C). As shown in the height profile of AFM

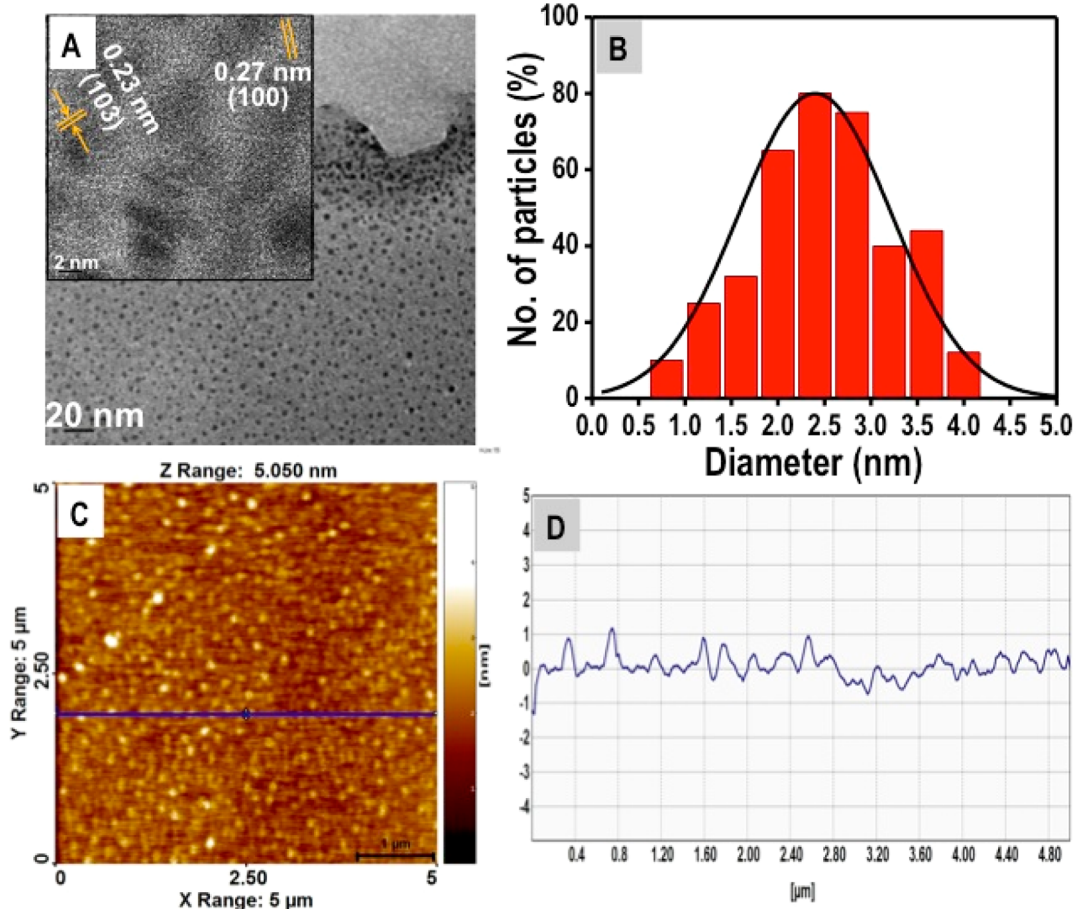


Figure 2. (A) TEM image of MoS_2 quantum dots interspersed in MoS_2 nanosheets. MoS_2 quantum dots of size ~ 2 nm are clearly seen. Inset shows the HRTEM image of MoS_2 quantum dots, showing the respective lattice spacing. In (B), the particle size distributions of MoS_2 quantum dots are shown. (C and D) AFM image and height profile of the MoS_2 quantum dots confirming a thickness of ~ 1 nm.

(Figure 2D), particles of uniform thickness of ~ 1 nm are observed, indicating monolayer structure of MoS_2 quantum dots, which are interspersed in few layer thick MoS_2 nanosheets. Energy-dispersive X-ray spectroscopy (EDX) measurements further confirmed the presence of Mo and S (Figure S3, Supporting Information). In order to further understand the phase composition, X-ray photoelectron spectroscopy (XPS) measurements were carried out and Mo 3d, S 2s, and S 2p regions were analyzed (Figure S4, Supporting Information). Peaks around 229.8 and 232.8 eV respectively correspond to the Mo^{4+} 3d_{5/2} and Mo^{4+} 3d_{3/2}, while the peaks at 163.8 and 162.6 eV correspond to S 2p_{1/2} and S 2p_{3/2} orbitals of divalent sulfide ions, which is in good agreement with the binding energies of Mo^{4+} and S^{2-} ions in 2H phase of MoS_2 .²⁵ A small peak appearing at 236 eV is an indication of slight oxidation of Mo from the 4+ state in MoS_2 to 6+.

Further structural characterization was studied by measuring the absorption spectra of the heterodimensional nanostructured MoS_2 sample (Figure 3A). The peaks at 395, 450, 610, and 660 nm are the characteristic absorption bands of exfoliated MoS_2 in the

solution.^{10,26,27} The excitonic peaks at 610 nm (A) and 660 nm (B), arising from the *K* point of the Brillouin zone are also clearly observed. The threshold at ~ 395 nm (C) and ~ 450 nm (D) could be assigned to the direct transition from the deep valence band to the conduction band.^{28,29} The absorption peaks in the near-UV region ($\lambda < 300$ nm) can be attributed to the excitonic features of MoS_2 quantum dots in the sample.²⁶ The direct excitonic transitions at the *K* point of the Brillouin zone are also reflected in photoluminescence spectra of exfoliated MoS_2 nanosheets, which exhibit the characteristic emission peaks at ~ 627 and ~ 670 nm (Figure 3B). For excitation at $\lambda = 500$ nm, which is approximately near the absorption threshold at ~ 450 nm, a single broad PL peak at ~ 570 nm is observed. This PL peak can be associated with the surface recombination that is seen in quantum-confined MoS_2 quantum dots.³⁰ The inset of Figure 3B shows the excitation-dependent luminescence spectra that confirm the presence of polydisperse MoS_2 quantum dots. The presence of many trap states may also contribute toward the excitation-dependent emission of the fluorescent MoS_2 quantum dots as observed in graphene quantum

dots.^{31,32} The lifetime measurement of the exfoliated MoS₂ hybrid nanomaterial confirms the existence of

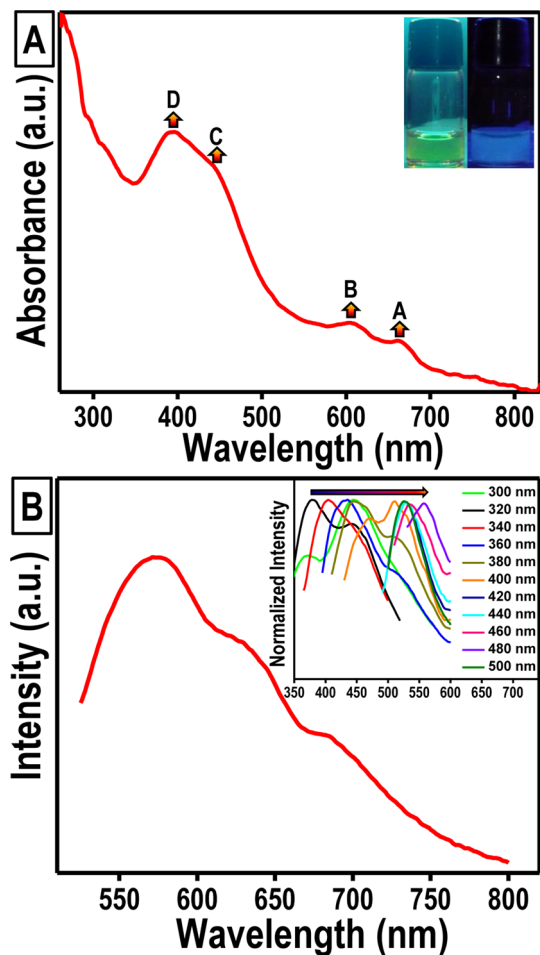


Figure 3. (A) UV-vis absorption spectrum of MoS₂ hybrid nanostructures in NMP. A photograph under visible and UV irradiation is shown in the inset. (B) Photoluminescence spectra of MoS₂ quantum dot-interspersed MoS₂ nanosheets recorded at an excitation wavelength of 400 nm. The characteristic peaks of MoS₂ nanosheets at ~ 627 and ~ 680 nm are clearly seen. The inset shows the excitation-dependent luminescence indicating the polydisperse nature of MoS₂ quantum dots.

different species (Figure S5, Supporting Information). Powder X-ray diffraction (XRD) and Raman spectroscopy measurements were carried out for further phase confirmation (Figure 4). The appearance of a strong (002) reflection²⁴ in the XRD pattern confirms the presence of exfoliated MoS₂ nanosheets with good crystallinity (Figure 4A). The XRD pattern of bulk MoS₂ was also compared, and all the reflections have been indexed (ICDD ref no. 04-003-3374). Figure 4B shows the characteristic Raman shifts near 382 and 407 cm⁻¹, corresponding to the E_{2g}^1 and A_{1g} active modes, respectively, indicating the presence of exfoliated MoS₂ nanostructures.³³⁻³⁵

Formation of these heterodimensional MoS₂ nanostructures can be understood from the sonication-induced scission of the bulk MoS₂ flakes. Here, the sonication conditions have been controlled to obtain MoS₂ quantum dot-interspersed MoS₂ nanosheets. The standing waves produced during ultrasonic treatment are believed to vibrate the lamellar particles, and, prolonged vibration results in the formation of quantum dots along with MoS₂ nanosheets, as observed in the TEM images (Figure 2A). Hence a simple combination of bath sonication followed by probe sonication of bulk MoS₂ flakes in NMP gives relatively large exfoliated sheets, with high concentration. A control experiment carried out by sonicating bulk MoS₂ in NMP using a probe sonicator alone for 7 h resulted in the formation of ultrathin MoS₂ sheets of varying sizes (Figure S2B, Supporting Information). However, there was no formation of MoS₂ quantum dots. Thus, the incorporation of bath sonication preceding the probe sonication leads to the formation of quantum dots along with ultrathin sheets of MoS₂. The initial bath sonication leads to the breakdown of bulk MoS₂ into smaller particles, which along with the bulk flakes get exfoliated on further sonication using an ultrasound horn (probe sonication), thus obtaining highly dispersed quantum dot-interspersed MoS₂ ultrathin sheets in NMP.

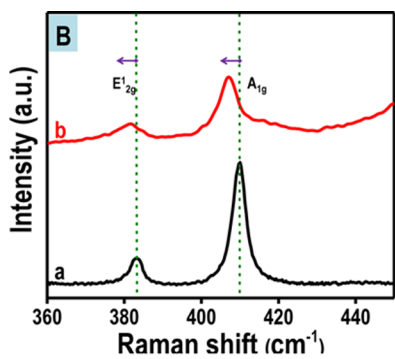


Figure 4. (A) XRD patterns of bulk MoS₂ (a) and MoS₂ quantum dot-interspersed MoS₂ nanosheets, exhibiting only the (002) plane (b). (B) Raman spectra recorded using a 536 nm laser for (a) bulk MoS₂ and (b) MoS₂ quantum dot-interspersed MoS₂ nanosheets, where the broadening of the peaks (E_{2g}^1 and A_{1g}) and peak shift indicate the decrease in the number of layers.

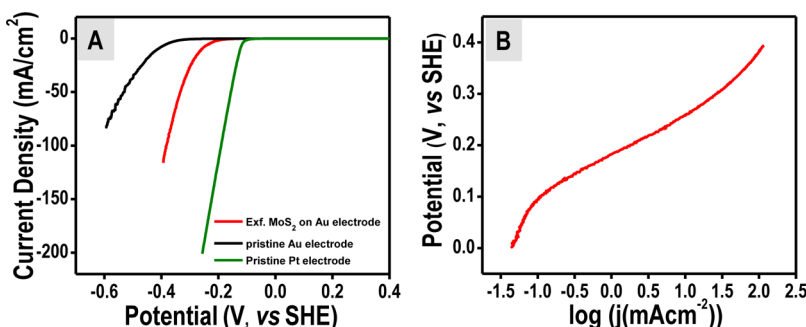


Figure 5. HER studies. (A) Polarization curves of the bare Au electrode, bare Pt, and MoS₂ hybrid nanostructures loaded on the Au electrode obtained in 0.5 M H₂SO₄ at a scan rate of 2 mV/s. (B) Tafel plot of the MoS₂ hybrid nanostructure loaded on the Au electrode.

The quantity of exfoliated material obtained in several of the liquid-based exfoliation routes is very low, which remains a big challenge for a range of practical applications that require large quantities of material, for example, energy applications.³⁶ Efforts have been undertaken to improve the dispersion concentration and flake size of exfoliated MoS₂ material by appropriate selection of the solvent. *N*-Methylpyrrolidone, with a surface energy of \sim 70 mJ m⁻², has been reported to give the maximum dispersion of exfoliated MoS₂.¹⁸ It is found that the stability of the dispersion containing exfoliated MoS₂ is maximum when the surface energy of the solvent matches that of nanosheets. However, the extraction of exfoliated MoS₂ from NMP through slow evaporation and heating leads to its aggregation and restacking. Here, through a novel and simple approach, the exfoliated material containing MoS₂ quantum dots interspersed in MoS₂ nanosheets was extracted in powder form (Figure S6, Supporting Information). With an excess of the less polar solvent, for instance, chloroform, when added to the NMP solvent containing our nanostructured MoS₂, it is found that the exfoliated material starts to precipitate and forms a layer at the top. This could be separated, washed with ethanol, and finally centrifuged to obtain the material in powder form, in relatively large quantities. The obtained powder is well characterized, and the exfoliated MoS₂ retains its morphology without any aggregation or restacking (Figure S6, Supporting Information).

The presence of active edge surfaces in MoS₂ nanostructures makes it an efficient and viable catalyst for hydrogen evolution reaction. Here we show the enhancement in the hydrogen evolution due to active participation of both MoS₂ quantum dots and nanosheets as electrocatalysts. HER measurements with these heterodimensional nanostructured MoS₂ were carried out using a three-electrode cell with 0.5 M sulfuric acid as electrolyte. Exfoliated MoS₂ material loaded on a Au electrode exhibited good electrocatalytic activity with a low onset potential of \sim 190 mV, where the hydrogen evolution was significantly observed (Figure 5A). The current density steadily

improved and reached a value of 120 mA/cm² at -0.4 V vs SHE, which is high compared to the bare Au electrode. The enhanced electrocatalytic activity was further supported from the calculated slope of the Tafel plots. A low Tafel slope of \sim 74 mV per decade with an exchange current density of 3.2×10^{-5} A cm⁻² indicates enhanced reaction kinetics (Figure 5B). To further investigate the catalytic activity, turnover frequency (TOF) has been estimated by calculating the number of active sites from the cyclic voltammogram^{14,37} (Figure S7, Supporting Information). A TOF of 0.013 s⁻¹ at $\eta = 0$ mV vs SHE has been observed (Figure S8, Supporting Information), which is very close to the reported value for MoS₂ nanoparticle based electrodes.³⁸ The large exchange current density could be attributed to the improved electron transfer rate, resulting from the large surface area of both MoS₂ quantum dots and nanosheets. Enhanced HER catalytic activity results from the enhanced edge to plane ratio. The heterodimensional hybrid material has two advantageous peculiarities, both resulting in an enhanced edge to basal plane ratio. First, slight oxidation as indicated in the XPS data can improve the density of the active sites, which helps to enhance the catalytic activity of MoS₂. Second, a relatively high order of stacking in the heterodimensional morphology when compared to the MoS₂ nanosheet also contributes toward the improved HER activity.¹⁴

CONCLUSION

In conclusion, we have demonstrated a simple technique to fabricate heterodimensional hybrid nanostructures of MoS₂ quantum dots interspersed in few-layer MoS₂ nanosheets, using a liquid phase exfoliation method. The larger concentration of active edges resulting from this unique morphology of MoS₂ nanostructures resulted in enhanced HER activity, showing low onset potential, along with large exchange current density. Moreover, we also showed novel approaches to extract these materials in powder form to realize its practical applications. The method can easily be scaled up to give a larger yield of high concentration dispersion of MoS₂ quantum

dots interspersed in thin MoS₂ nanosheets. We believe the same technique can be adapted to other layered materials, which opens up the route for large-scale

synthesis of tailored heterodimensional nanostructures that can find use as high-performance electrodes for energy applications.

METHODS

Liquid Exfoliation of MoS₂. A highly disperse suspension of MoS₂ quantum dot interspersed in few-layered MoS₂ nanosheets was prepared using a simple liquid exfoliation technique involving bath sonication followed by ultrasound probe sonication of MoS₂ flakes (Sigma-Aldrich) in 1 methyl-2-pyrrolidone. In short, 100 mg of MoS₂ powder (Sigma-Aldrich) was added to 10 mL of 1-methyl-2-pyrrolidone in a 20 mL beaker and sonicated in an ultrasonic bath continuously for 3.5 h. Then, the dispersion was sonicated with a sonic tip for another 3.5 h. The dispersion was kept undisturbed overnight, and the top two-thirds was centrifuged at 5500 rpm for 90 min. The bath temperature was kept below 277 K by keeping the sample in an ice bath.

Physical Characterizations. The highly stable dispersion was decanted and characterized using various experimental tools. Scanning electron microscope (SEM) imaging was performed using a Nova NanoSEM 450, an FEI coupled with an Apollo X EDAX, and a field emission transmission electron microscope (FEI Technic 300). X-ray photoelectron spectroscopy measurements were carried out using an Omicron ESCA probe spectrometer with polychromatic Mg K α X-rays ($h\nu = 1253.6$ eV). The diffraction patterns were collected using an Emperean PAAnalytical XRD system with reference X-ray illumination as Cu K α radiation at 0.154 nm. Raman measurements with the excitation laser line of 632.8 nm were performed using a LabRAM HR Raman spectrometer (Horiba Jobin Yvon). Absorption spectra were collected using a Shimadzu UV-3600 UV-vis-NIR spectrophotometer. High-resolution transmission electron microscopy images were taken in a JEOL JEM 2100 (200 kV) with a LaB₆ electron gun, and AFM data were obtained in a Veeco Multimode 8 with a Nanoscope V in contact mode to observe heterodimensional nanostructures of MoS₂ quantum dot-interspersed few-layered MoS₂ nanosheets.

Electrochemical Measurements. A bare Au electrode with a diameter of 0.49 mm was polished using Al₂O₃ and cleaned with distilled water through sonication for 5 min. Then the surface of the electrode was cleaned by applying a potential of 0.2 to 1.5 V (vs SHE) at a scan rate of 300 mV/s continuously for 300 cycles. Later the Au electrode was washed with distilled water and dried under vacuum at 85 °C. The electrode was then dipped into fresh MoS₂ solution and kept undisturbed for 24 h at room temperature. The catalytic activity of the MoS₂-loaded and bare Au electrode was tested in 0.5 M H₂SO₄ with a three-electrode system. Pt and Ag/AgCl were taken as the counter and reference electrode, respectively. The potential applied was about OCP to -0.8.

Conflict of Interest: The authors declare no competing financial interest.

Acknowledgment. This work has been partially supported by the Board of Research in Nuclear Sciences (BRNS), Department of Atomic Energy (DAE), Govt. of India, through a DAE Young Scientist Research Award (No. 2012/20/34/5/BRNS). The authors gratefully acknowledge Dr. Vijayamohanan K. Pillai for several fruitful discussions. We are thankful to Mr. N. Sreekanth and Mr. Naresh Kumar for helpful discussions. D.D. acknowledges CSIR, Govt. of India, for the research fellowship.

Supporting Information Available: The SEM images of the exfoliated MoS₂, EDAX spectrum showing the presence of Mo and S, additional TEM images of the control experiments, XPS data for Mo and S, showing the slight oxidation, and lifetime measurements. Photograph of the extraction of exfoliated samples and their TEM images. Estimation of TOF. This material is available free of charge via the Internet at <http://pubs.acs.org>.

REFERENCES AND NOTES

- Zhou, K.-G.; Mao, N.-N.; Wang, H.-X.; Peng, Y.; Zhang, H.-L. A Mixed-Solvent Strategy for Efficient Exfoliation of Inorganic Graphene Analogues. *Angew. Chem., Int. Ed.* **2011**, *50*, 10839–10842.
- Chhowalla, M.; Shin, H. S.; Eda, G.; Li, L.-J.; Loh, K. P.; Zhang, H. The Chemistry of Two-Dimensional Layered Transition Metal Dichalcogenide Nanosheets. *Nat. Commun.* **2013**, *5*, 263–275.
- Geim, A. K. Graphene: Status and Prospects. *Science* **2009**, *324*, 1530–1534.
- Geim, A. K.; Novoselov, K. S. The Rise of Graphene. *Nat. Mater.* **2007**, *6*, 183–191.
- Ibrahem, M. A.; Lan, T.-w.; Huang, J. K.; Chen, Y.-Y.; Wei, K.-H.; Li, L.-J.; Chu, C. W. High Quantity and Quality Few-Layers Transition Metal Disulfide Nanosheets from Wet-Milling Exfoliation. *RSC Adv.* **2013**, *3*, 13193–13202.
- Huang, X.; Zeng, Z.; Zhang, H. Metal Dichalcogenide Nanosheets: Preparation, Properties and Applications. *Chem. Soc. Rev.* **2013**, *42*, 1934–1946.
- Mak, K. F.; Lee, C.; Hone, J.; Shan, J.; Heinz, T. F. Atomically Thin MoS₂: A New Direct-Gap Semiconductor. *Phys. Rev. Lett.* **2010**, *105*, 136805 1–4.
- Yao, Y.; Tolentino, L.; Yang, Z.; Song, X.; Zhang, W.; Chen, Y.; Wong, C.-p. High-Concentration Aqueous Dispersions of MoS₂. *Adv. Funct. Mater.* **2013**, *23*, 3577–3583.
- Wang, H.; Lu, Z.; Xu, S.; Kong, D.; Cha, J.-J.; Zheng, G.; Hsu, P.-C.; Yan, K.; Bradshaw, D.; Prinz, F. B.; Cui, Y. Electrochemical Tuning of Vertically Aligned MoS₂ Nanofilms and Its Application in Improving Hydrogen Evolution Reaction. *Proc. Natl. Acad. Sci. U.S.A.* **2013**, *110*, 19701–19706.
- Wang, T.; Liu, L.; Zhu, Z.; Papakonstantinou, P.; Hu, J.; Liu, H.; Li, M. Enhanced Electrocatalytic Activity for Hydrogen Evolution Reaction from Self-Assembled Monodispersed Molybdenum Sulfide Nanoparticles on an Au Electrode. *Energy Environ. Sci.* **2013**, *6*, 625–633.
- Lu, Z.; Zhang, H.; Zhu, W.; Yu, X.; Kuang, Y.; Chang, Z.; Lei, X.; Sun, X. *In Situ* Fabrication of Porous MoS₂ Thin-Films as High-Performance Catalysts for Electrochemical Hydrogen Evolution. *Chem. Commun.* **2013**, *49*, 7516–7518.
- Laursen, A. B.; Kegnaes, S.; Dahl, S.; Chorkendorff, I. Molybdenum Sulfides-Efficient and Viable Materials for Electro and Photoelectrocatalytic Hydrogen Evolution. *Energy Environ. Sci.* **2012**, *5*, 5577–5591.
- Li, Y.; Wang, H.; Xie, L.; Liang, Y.; Hong, G.; Dai, H. MoS₂ Nanoparticles Grown on Graphene: An Advanced Catalyst for the Hydrogen Evolution Reaction. *J. Am. Chem. Soc.* **2011**, *133*, 7296–7299.
- Wu, Z.; Fang, B.; Wang, Z.; Wang, C.; Liu, Z.; Liu, F.; Wang, W.; Alfantazi, A.; Wang, D.; Wilkinson, D. P. MoS₂ Nanosheets: A Designed Structure with High Active Site Density for the Hydrogen Evolution Reaction. *ACS Catal.* **2013**, *3*, 2101–2107.
- Vrubel, H.; Hu, X. Growth and Activation of an Amorphous Molybdenum Sulfide Hydrogen Evolving Catalyst. *ACS Catal.* **2013**, *3*, 2002–2011.
- Voiry, D.; Salehi, M.; Silva, R.; Fujita, T.; Chen, M.; Asefa, T.; Shenoy, V. B.; Eda, G.; Chhowalla, M. Conducting MoS₂ Nanosheets as Catalysts for Hydrogen Evolution Reaction. *Nano Lett.* **2013**, *13*, 6222–6227.
- Yin, Z.; Li, H.; Li, H.; Jiang, L.; Shi, Y.; Sun, Y.; Lu, G.; Zhang, Q.; Chen, X.; Zhang, H. Single-Layer MoS₂ Phototransistors. *ACS Nano* **2011**, *6*, 74–80.
- Cunningham, G.; Lotya, M.; Cucinotta, C. S.; Sanvito, S.; Bergin, S. D.; Menzel, R.; Shaffer, M. S. P.; Coleman, J. N. Solvent Exfoliation of Transition Metal Dichalcogenides: Dispersibility of Exfoliated Nanosheets Varies Only Weakly between Compounds. *ACS Nano* **2012**, *6*, 3468–3480.

19. Coleman, J. N.; Lotya, M.; O'Neill, A.; Bergin, S. D.; King, P. J.; Khan, U.; Young, K.; Gaucher, A.; De, S.; Smith, R. J.; Shvets, I. V.; *et al.* Two-Dimensional Nanosheets Produced by Liquid Exfoliation of Layered Materials. *Science* **2011**, *331*, 568–571.
20. Zeng, Z.; Sun, T.; Zhu, J.; Huang, X.; Yin, Z.; Lu, G.; Fan, Z.; Yan, Q.; Hng, H. H.; Zhang, H. An Effective Method for the Fabrication of Few-Layer-Thick Inorganic Nanosheets. *Angew. Chem., Int. Ed.* **2012**, *51*, 9052–9056.
21. Lee, Y.-H.; Zhang, X.-Q.; Zhang, W.; Chang, M.-T.; Lin, C.-T.; Chang, K.-D.; Yu, Y.-C.; Wang, J. T.-W.; Chang, C.-S.; Li, L.-J.; Lin, T.-W. Synthesis of Large-Area MoS_2 Atomic Layers with Chemical Vapor Deposition. *Adv. Mater.* **2012**, *24*, 2320–2325.
22. Najmaei, S.; Liu, Z.; Zhou, W.; Zou, X.; Shi, G.; Lei, S.; Yakobson, B. I.; Idrobo, J.-C.; Ajayan, P. M.; Lou, J. Vapour Phase Growth and Grain Boundary Structure of Molybdenum Disulphide Atomic Layers. *Nat. Mater.* **2013**, *12*, 754–759.
23. O'Neill, A.; Khan, U.; Coleman, J. N. Preparation of High Concentration Dispersions of Exfoliated MoS_2 with Increased Flake Size. *Chem. Mater.* **2012**, *24*, 2414–2421.
24. Stengl, V.; Henych, J. Strongly Luminescent Monolayered MoS_2 Prepared by Effective Ultrasound Exfoliation. *Nanoscale* **2013**, *5*, 3387–3394.
25. Eda, G.; Yamaguchi, H.; Voiry, D.; Fujita, T.; Chen, M.; Chhowalla, M. Photoluminescence from Chemically Exfoliated MoS_2 . *Nano Lett.* **2011**, *11*, 5111–5116.
26. Chikan, V.; Kelley, D. F. Size-Dependent Spectroscopy of MoS_2 Nanoclusters. *J. Phys. Chem. B* **2002**, *106*, 3794–3804.
27. Wilcoxon, J. P.; Newcomer, P. P.; Samara, G. A. Synthesis and Optical Properties of MoS_2 and Isomorphous Nanoclusters in the Quantum Confinement Regime. *J. Appl. Phys.* **1997**, *81*, 7934–7944.
28. Wilson, J. A.; Yoffe, A. D. The Transition Metal Dichalcogenides Discussion and Interpretation of the Observed Optical, Electrical and Structural Properties. *Adv. Phys.* **1969**, *18*, 193–335.
29. Wilcoxon, J. P.; Samara, G. A. Strong Quantum-Size Effects in a Layered Semiconductor: MoS_2 Nanoclusters. *Phys. Rev. B, PRB* **1995**, *51*, 7299–7302.
30. Wilcoxon, J. P.; Newcomer, P. P.; Samara, G. A. Synthesis and Optical Properties of MoS_2 Nanoclusters. *Mater. Res. Soc. Symp. Proc.* **1996**, *452*, 371–376.
31. Bao, L.; Zhang, Z.-L.; Tian, Z.-Q.; Zhang, L.; Liu, C.; Lin, Y.; Qi, B.; Pang, D.-W. Electrochemical Tuning of Luminescent Carbon Nanodots: From Preparation to Luminescence Mechanism. *Adv. Mater.* **2011**, *23*, 5801–5806.
32. Shinde, D. B.; Pillai, V. K. Electrochemical Preparation of Luminescent Graphene Quantum Dots from Multiwalled Carbon Nanotubes. *Chem.—Eur. J.* **2012**, *18*, 12522–12528.
33. Li, H.; Zhang, Q.; Yap, C. C. R.; Tay, B. K.; Edwin, T. H. T.; Olivier, A.; Baillargeat, D. From Bulk to Monolayer MoS_2 : Evolution of Raman Scattering. *Adv. Funct. Mater.* **2012**, *22*, 1385–1390.
34. Sreeprasad, T. S.; Nguyen, P.; Kim, N.; Berry, V. Controlled, Defect-Guided, Metal-Nanoparticle Incorporation onto MoS_2 via Chemical and Microwave Routes: Electrical, Thermal, and Structural Properties. *Nano Lett.* **2013**, *13*, 4434–4441.
35. Zeng, Z.; Yin, Z.; Huang, X.; Li, H.; He, Q.; Lu, G.; Boey, F.; Zhang, H. Single-Layer Semiconducting Nanosheets: High-Yield Preparation and Device Fabrication. *Angew. Chem., Int. Ed.* **2011**, *50*, 11093–11097.
36. Winchester, A.; Ghosh, S.; Feng, S.; Elias, A. L.; Mallouk, T.; Terrones, M.; Talapatra, S. Electrochemical Characterization of Liquid Phase Exfoliated Two-Dimensional Layers of Molybdenum Disulfide. *ACS Appl. Mater. Interfaces* **2014**, *6*, 2125–2130.
37. Merki, D.; Fierro, S.; Vrubel, H.; Hu, X. Amorphous Molybdenum Sulfide Films as Catalysts for Electrochemical Hydrogen Production in Water. *Chem. Sci.* **2011**, *2*, 1262–1267.
38. Jaramillo, T. F.; Jørgensen, K. P.; Bonde, J.; Nielsen, J. H.; Horch, S.; Chorkendorff, I. Identification of Active Edge Sites for Electrochemical H_2 Evolution from MoS_2 Nanocatalysts. *Science* **2007**, *317*, 100–102.